From Shortest-path to All-path: The Routing Continuum Theory and its applications (Supplementary Materials)

Yanhua Li, *Member, IEEE,* Zhi-Li Zhang, *Fellow, IEEE,* and Daniel Boley, *Member, IEEE*

Abstract—This documents provides numerical illustration results obtained by applying the routing continuum theory in two synthetic networks and a real network topology. Moreover, besides the generalizations of the mixed L_1- and L_2-norm network flow optimization problem discussed in the main file, in this document, we discuss one more application in analyzing network robustness, by introducing the generalized shortest path and random walk betweenness centrality measures.

Index Terms—Routing continuum, network flow, betweenness centrality.

1 Numerical Illustration of Routing Continuum Theory

We use two synthetic networks and a real network to show how the routing continuum grows as the parameter θ changes. Fig. 1 shows an example topology, with three disjoint paths between the source 1 and the destination 5, and each link is with 1-unit weight. As the parameter $\theta \geq 0$ increases, the longer paths $P3 = \{1 \to 3 \to 4 \to 5\}$ and $P2 = \{1 \to 2 \to 5\}$ are truncated gradually, and the shortest path $P1 = \{1 \to 5\}$ is obtained when θ increases to 1. Fig. 2 shows the routing continuum, i.e. the optimal flow distributions at each θ. We see that within the interval $\theta \in [0, 0.4]$, the flows on the longer paths $P2$ and $P3$ get linearly redistributed to the shortest path $P1$, and the longest path $P3$ gets truncated when $\theta = 0.4$. Then the flow of the second longest path $P2$ keeps decreasing as θ increases, until the second boundary condition $\theta = 1$ holds, where $P2$ is truncated. During the routing evolution process, the network flows are always redistributed from longer paths to the shorter path, while increasing θ. When $\theta > 1$, namely, the largest boundary condition, the routing solution is stabilized to the shortest path, i.e. $P1$.

Fig. 3 shows another example with five connected nodes in the topology. Weights w_{ij}'s are marked on the links. The flow initiates at source 1 and is removed from destination 5. Fig. 4~Fig. 8 show the optimal flow distributions (marked on individual links) under five boundary conditions, $[\theta_0 = 0, \theta_1 = 0.0914, \theta_2 = 0.2850, \theta_3 = 0.5700, \theta_4 = 2]$, In Fig. 4($\theta_0 = 0$), every link is active and follows the potential based "all-path" routing. Then, as θ increases to $\theta_1 = 0.0914$ (in Fig.5), link $(1, 4)$ is truncated, and within the interval $\theta \in [0, \theta_1]$, only the flow on path $\{1 \to 4 \to 5\}$ decreases, and gets redistributed to other paths, because this path with total length 11 is the longest path in $\mathcal{P}(0)$, i.e. the "all-path" routing graph. Then, when θ increases to $\theta_2 = 0.2850$, the flows on links $(2, 3)$ and $(3, 5)$ are truncated, because these two links are on the second longest path $\{1 \to 2 \to 3 \to 5\}$, with path length 5. Similarly, when θ keeps increasing to θ_3 and θ_4, the rest two longer paths $\{1 \to 2 \to 5\}$ and $\{1 \to 2 \to 4 \to 5\}$ get removed, respectively, and only the shortest path $\{1 \to 5\}$ is left at last.

Now, we apply the routing continuum theory to Internet2 Abilene Network [1]. The Abilene network was a high-performance backbone network established by the Internet2 community in the late 1990s. The Abilene Network was retired and became the "Internet2 Network" in 2007. Fig. 15 shows its 11 regional network aggregation points and backbone connections across them (primarily OC192 or OC48 backbone). We consider the transmission cost between two end points roughly proportional to their actual geographic distance, because the velocity of light in an optical fiber becomes 60-70% compared to it in vacuum [13], [26], [33]. Hence, in the numerical analysis, we simply use the geographical distance as the link weight for the transmission cost as marked in Fig. 9. We choose the flow demand from `Sunnyvale` to `New York`. As we increase θ from 0, we observe a sequence of five boundary θ's, i.e., $[\theta_0 = 0, \theta_1 = 0.1082, \theta_2 = 0.2498, \theta_3 = 0.4943, \theta_4 = 3.2108]$, in which order links $(4 \to 6)$, $(5 \to 1)$, $(10 \to 9 \to 3)$ and $(10 \to 7 \to 4 \to 1 \to 11 \to 8)$ get truncated in sequence, and the optimal flow distribution evolves from the "all-path" routing to "shortest-path" routing. When $\theta_0 = 0$, all paths are present in delivering the contents, whereas only the shortest path $\{10 \to 3 \to 6 \to 5 \to 2 \to 8\}$ is active for $\theta \geq 3.2108$.

2 Network Robustness Analysis via Generalized Centrality Measure

The optimal flow distribution $X^*(\theta)$ to the mixed L_1- and L_2-norm network flow optimization problem indicates exactly the loads on each link (resp. node) for certain flow demands. When considering flow demands from all source

- *This work was supported in part by the NSF grants CNS-1017092 and IIS-0916750, the DTRA grant HDTRA1-09-1-0050. An earlier version of this work appeared in the Proceedings of IEEE ICDCS [22], June 2011.*
Yanhua Li is with HUAWEI Noah's Ark Lab, China. Zhi-Li Zhang and Daniel Boley are with the Department of Computer Science and Engineering, University of Minnesota, Twin Cities, Minneapolis, MN, 55455.
E-mail: {yanhua,zhzhang,boley}@cs.umn.edu

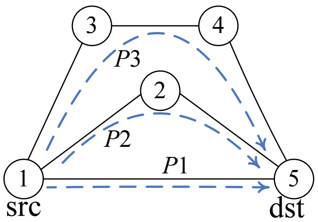

Fig. 1. Example 1 with uniform weight $w_{ij} = 1$

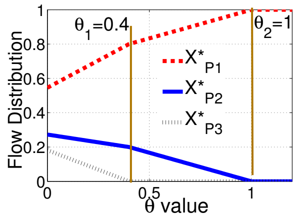

Fig. 2. Flow distribution evolution of graph Fig. 1

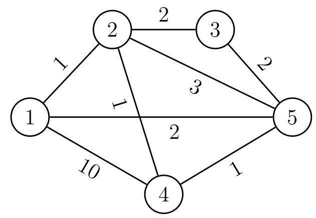

Fig. 3. Example 2: Weight Graph

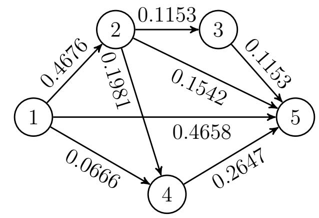

Fig. 4. Flow distribution, $\theta_0 = 0$

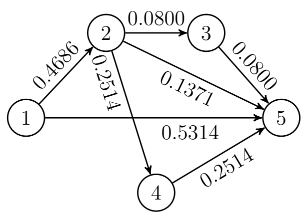

Fig. 5. Flow distribution with $\theta_1 = 0.0914$

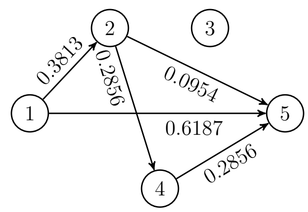

Fig. 6. Flow distribution with $\theta_2 = 0.2850$

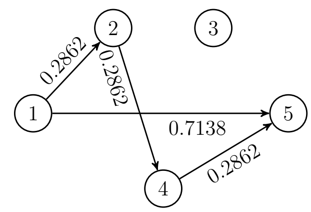

Fig. 7. Flow distribution with $\theta_3 = 0.5700$

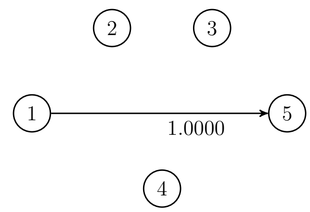

Fig. 8. Flow distribution with $\theta_4 = 2$

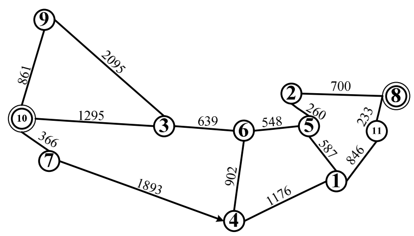

Fig. 9. Weights on the Abilene network

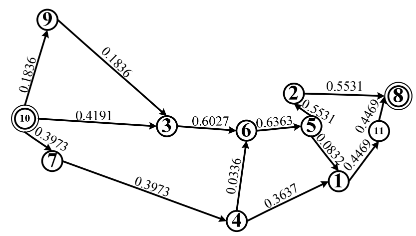

Fig. 10. Flow distribution $\theta_0 = 0$

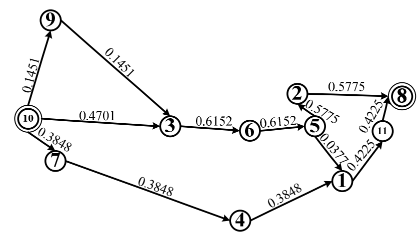

Fig. 11. Flow distribution $\theta_1 = 0.1082$

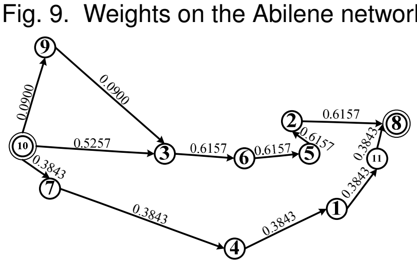

Fig. 12. Flow distribution $\theta_1 = 0.2498$

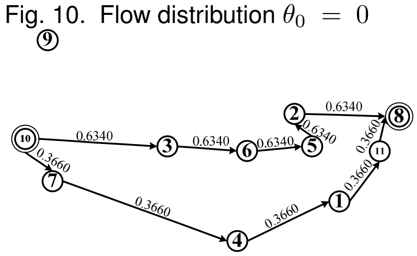

Fig. 13. Flow distribution $\theta_3 = 0.4943$

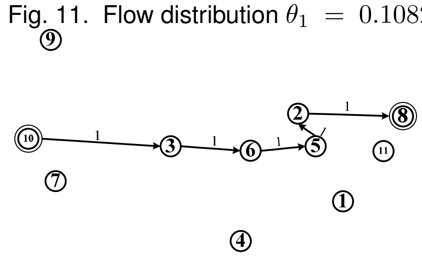

Fig. 14. Flow distribution $\theta_4 = 3.2108$

destination pairs, the average network flow on each link (resp. node) infers the "importance" of the link (resp. node), namely, the influence of the link (resp. node) in case of failure or being attacked, which in turn reveals the robustness structure of networks, i.e., which area of the network is more vulnerable to attacks. The robustness centrality measure of links and nodes in the network has been extensively studied, and has been applied to design topology control algorithm and routing protocol in wireless sensor networks and delay tolerant networks [14], [19]. Below, we show how our routing continuum theory can be used to generalize various robustness centrality measures of links/nodes in networks, where the ranking of links/nodes in terms of their betweenness infer the network robustness structure, i.e., those areas with high betweenness links/nodes expose more risks to attacks or failures, as when removing these links/nodes, more flows have to be rerouted or failed.

2.1 Centrality measures for mixed network flow

Centrality measures were first developed in social network analysis [9], [25], for example, how influential a user is in a social network, with applications in robust community detection [18], [23], mobility prediction [5], and etc. There are four widely used centrality measures [25], that capture the relative importance of a vertex or an edge within a network from various aspects: *degree* [1], *eigenvector centrality* [2], *betweenness* [10], [16], and *closeness* [28]. Betweenness and closeness centrality measures are directly interpretable in

1. The node degree centrality is simply defined as the number of links associated with a node, which reflects locally (i.e., within one hop,) how well the node is connected to other nodes.

2. Eigenvector centrality takes the leading Eigenvector, i.e., the Eigenvector corresponding to the largest Eigenvalue, of the adjacent matrix A as relative scores to all nodes in the network, which follows the concept that connections to nodes with higher scores contribute more to the score of the node than connections to nodes with lower scores. PageRank [27] and Katz centrality [20] can be viewed as two variations of the Eigenvector centrality measure.

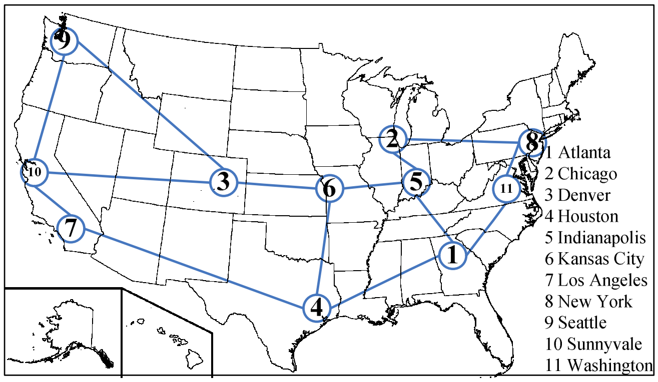

Fig. 15. Abilene network topology

terms of the shortest path and all-path routing, thus can be generalized using our routing continuum theory to account for mixed network flows. In the following, we will introduce the mixed-flow betweenness for nodes or edges, a natural generalization of the existing betweenness centrality measures. The mixed-flow betweenness measures indicate the importance of nodes or edges in terms of the degree to which a node or an edge is participating in the communication between node pairs in the network, which has implications in network resource relocations and detecting robust subgraphs that are resilient to attacks and failures. Note that closeness centrality can similarly be generalized, and we omit these results here for brevity.

2.2 Node Betweenness centrality

Node betweenness has been studied in the past as a measure of the centrality and influence of nodes in networks.

Shortest-path betweenness. A simple example of such a betweenness measure initially proposed by Freeman [8], [16], [17] is shortest-path betweenness. Given a node i, its shortest-path betweenness is defined as the number of shortest (geodesic) paths between pairs of all other nodes that run through i. To be precise, given a graph $G = (V, E)$, node i's betweenness centrality [16], [17] C_i^S is defined as[3]

$$C_i^S = \frac{2\sum_{s<t\in V} g_i^{(st)}}{n(n-1)}, \tag{1}$$

where $g_i^{(st)}$ is the number of shortest paths from node s to node t that pass through i. Since the graph is undirected, $g_i^{(st)} = g_i^{(ts)}$ always holds, thus computing $g_i^{(st)}$ for only half of all node pairs (i.e., for $s < t$) is sufficient. If there is more than one shortest path between a node pair, each path is given equal weight such that the total weight of all of the paths is unity. Since when θ is large enough, the optimal flow distribution denoted by $X^*(\infty)$ represents the shortest path solution, the shortest path betweenness centrality C_i^S can be written as

$$C_i^S = \frac{2\sum_{s<t\in V}\sum_{k\in V} {X^{(st)}}^*_{ki}(\infty)}{n(n-1)}. \tag{2}$$

Current-flow betweeness[4]**.** Considering that the circuit created by placing a resister on each edge of the network and unit current source and destination at a particular node pair. The resulting current flow in the network will follow Kirchhoff's and Ohm's laws, going from source to destination along a multitude of paths. Hence, The current-flow betweenness [24] for a node i is defined as the absolute value of the currents summed over all node pairs that run through i. The optimal optimal flow distribution ${X^{(st)}}^*(0)$ of the L_2 norm flow optimization problem represents exactly the current flow for source destination pair (s, t) with $\theta = 0$. The current-flow betweenness C_i^C of node i can be written in terms of ${X^{(st)}}^*(0)$ as

$$C_i^C = \frac{2\sum_{s<t\in V}\sum_{k\in V} {X^{(st)}}^*_{ki}(0)}{n(n-1)}. \tag{3}$$

Mixed-flow betweeness. Shortest-path betweenness and current-flow betweenness present two extremes. One uses only shortest paths, and the other favors all-path to deliver network flow. Our routing continuum theory naturally leads to a generalized mix-flow betweenness, $C_i(\theta)$, which captures how much mixed flow $X^*(\theta)$ runs through a node given a flow combination parameter θ.

$$C_i(\theta) = \frac{2\sum_{s<t\in V}\sum_{k\in V} {X^{(st)}}^*_{ki}(\theta)}{n(n-1)}, \tag{4}$$

with $\theta \geq 0$. Note that the shortest-path betweenness (eq.(2)) and the current-flow betweenness (eq.(3)) are two special cases of mixed-flow betweenness, as $C_i^S = C_i(\infty)$ and $C_i^C = C_i(0)$, respectively. Given a specific $\theta \geq 0$, $C_i(\theta)$ captures the importance of node i, in terms of the average optimal flow going through node i over all source destination pairs.

2.3 Edge betweenness centrality

Analogically, the betweenness centrality can be defined for *edges*, capturing how much network flow going through a particular edge, summed over all node pairs in the network.

The *shortest-path betweenness* of an edge (i, j) is the total number of shortest paths running along (i, j), which was first introduced by Anthonisse in [6], and Newman formally defined it in [23]. It can be written in terms of the optimal shortest path flow distribution denoted by $X^*(\infty)$ as

$$C_{ij}^S = \frac{2\sum_{s<t\in V} {X^{(st)}}^*_{ij}(\infty)}{n(n-1)} \tag{5}$$

Similarly, the *current-flow betweenness* of an edge (i, j) is the current flow running along (i, j) [10], [23], which can be

3. Here, the normalizing constant is $n(n-1)$, where i may also be a start or end node of a source destination pair. Some definitions only count for those node pairs without i as a start or end node, where the normalizing constant becomes $(n-1)(n-2)$ instead.

4. Current-flow betweenness is proven to be equivalent to random walk (RW) betweenness [24]. For a node i, we calculate the expected number of times that a random walk between a particular node pair will pass through i, and RW betweenness is the summation over all node pairs.

computed using the following eq.(6) in terms of the optimal L_2 network flow distribution denoted by $X^*(0)$ as

$$C_{ij}^C = \frac{2\sum_{s<t\in V} {X^{(st)}}^*_{ij}(0)}{n(n-1)} \tag{6}$$

The mixed-flow betweenness of an edge (i, j) is then a natural generalization of eq.(5) and eq.(6) for $\theta \geq 0$.

$$C_{ij}(\theta) = \frac{2\sum_{s<t\in V} {X^{(st)}}^*_{ij}(\theta)}{n(n-1)} \tag{7}$$

As discussed earlier, the trade-off parameter $\theta \geq 0$ governs how much shortest path flow vs current flow is considered in the mixed flow optimization problem. The mixed-flow betweenness centrality measure for a link/node captures how crucial the link/node is in carrying the network flow for all possible node pairs. In communication networks, the link/node betweenness measures in fact indicate how much (mixed) network flow has to go through a particular link/node for all source-destination pairs. An attack or failure to the links/nodes with high betweenness leads to more influential impacts to the network traffic. Hence the ranking of the links/nodes in terms of their betweenness infer the network robustness structure, namely, areas with high betweenness links/nodes are more vulnerable to attacks or failures, since more flows have to be rerouted or failed if these links/nodes fail.

TABLE 1
Edge ranking in mixed-flow betweenness ($\theta \geq 0$).

Edge ranking	when $\theta \in [0, 0.002)$	when $\theta \in [0.002, 0.06)$	when $\theta \geq 0.06$
# 1	**(1,2)**	**(1,2)**	**(2,4)**
# 2	**(4,5)**	**(2,4)**	**(1,2)**
# 3	**(2,4)**	**(4,5)**	**(4,5)**
# 4	(2,3)	(2,3)	(2,3)
# 5	(3,5)	(3,5)	(3,5)
# 6	(1,5)	(1,5)	(1,5)
# 7	(2,5)	(2,5)	(2,5)
# 8	(1,4)	(1,4)	(1,4)

2.4 Numerical examples

Next, we use the topology in Fig. 3 and a real network topology, i.e., Internet2 Abilene Network [1], as examples, to show how the ranking of node/link in terms of betweenness changes over θ.

When computing the betweenness centrality measures for the five node topology in Fig. 3, we observe that as increasing $\theta \geq 0$, the ranking of links in terms of their mixed-flow betweenness keeps relatively robust, namely, there are only three different link ranking orders (See Tab 1). The highest betweenness links are $(1, 2)$, $(4, 5)$ and $(2, 4)$, which all have the smallest link weights. The link $(2, 4)$ steps up to the highest ranking, when $\theta \geq 0.06$. The node betweenness ranking is more stable, which is unchanged over θ's for topology in Fig. 3 with nodes ranked as $\{2, 5, 4, 1, 3\}$ in a decreasing order. Nodes with more links and lower link weights are ranked higher, since they are more likely to serve as hubs to carry more network flows.

Now we investigate how the link and node betweenness ranking vary over θ in Abilene network. As we increase $\theta \geq 0$, there are twelve boundary θ's, governing the different ranking of link betweenness in Abilene network as shown in Table 2. We observe that when θ changes, namely, the network flow evolves from "all-path" flow to "shortest-path" flow, the ranks of links with the highest betweeness keep high ranking over θ, i.e., links at rank # 1 to # 5 are unchanged. On the other hand, the betweenness centrality link $(3, 10)$ increases from the rank #11 to #6 gradually (as highlighted in Table 2), which happens because the high link weight of $(3, 10)$ suppress the "all-path (current)" flow going through it, but it resides on more shortest paths among node pairs, thus generates higher shortest-path flow when θ is large. Moreover, the ranks of links such as $(1, 11)$, $(2, 8)$, and $(8, 11)$ decrease as θ increases. The ranks of some other links, including $(1, 5)$ and $(4, 7)$, keep stable at rank #7-#9. When looking at the node betweenness, the ranking is more stable than links, which is unchanged for all θ's as shown in Table 3. The nodes placed in central US, such as `Kansas City` and `Indianapolis` posses highest node betweenness centrality, namely, being the busiest nodes in carrying network flow.

We also computed the ranking of link/node betweenness in other real networks, such as Roofnet [3] (with 38 nodes), CERNET [4] (with 36 nodes), GEANT [2] (with 23 nodes), where similar results are obtained and we omit them here for brevity. From all these results, the node betweenness centrality ranking is overall more stable than link betweenness centrality ranking, through the entire routing continuum, i.e., all $\theta \geq 0$.

3 Discussion

In a broader context, the mixed L_1/L_2 optimization formulation has been widely used, e.g., in the classical LASSO problems [30], namely, the least square optimization problems with a L_1-norm penalty term, and more recently, in compressive sensing [11], [31]. It is therefore well-known that the L_1-norm penalty forces the least-square solution, X^*, to meet certain sparsity constraints, i.e., $||X^*||_1 \leq \epsilon$. Compared with LASSO and compressive sensing settings, our setting has a set of additional flow conservation constraints — these are what makes the problem *unique* and leads to solutions that have interesting interpretations and consequences, where the solutions to the more general LASSO and compressive sensing settings may not have, *apart from the sparsity of the solutions*.

Indeed, our routing continuum theory and the mixed L_1- and L_2-norm flow optimiaztion can be interpreted in terms of the "sparsity" of the solutions also: the optimal flow solution $X^*(\theta)$ to the mixed L_1/L_2-norm flow optimization leads to a *sparser* routing graph, where the *path length* of routes used for routing the optimal flow from a source to a destination can not be $(1 + \theta^{-1})$ longer than the shortest paths. More surprising and interesting is that we can generate the *entire routing continuum* from the mixed L_1/L_2-norm flow optimization. The flow conservation constraints in fact play a key role here: it leads to the duality of the optimal flows, $X^*(\theta)$, a function defined on the *edges* of a network, and the optimal (*generalized*) potential functions, $U^*(\theta)$, a function defined on the *nodes* of a network. This allows us to solve $U^*(\theta)$ through

TABLE 2
Edge ranking in mixed-flow betweenness in Abilene network ($\theta \geq 0$).

θ	0	0.0535	0.0617	0.0647	0.0839	0.0918	0.0964	0.1079	0.1335	0.2650	0.2874	0.3176
# 1	(5,6)	(5,6)	(5,6)	(5,6)	(5,6)	(5,6)	(5,6)	(5,6)	(5,6)	(5,6)	(5,6)	(5,6)
# 2	(3,6)	(3,6)	(3,6)	(3,6)	(3,6)	(3,6)	(3,6)	(3,6)	(3,6)	(3,6)	(3,6)	(3,6)
# 3	(2,5)	(2,5)	(2,5)	(2,5)	(2,5)	(2,5)	(2,5)	(2,5)	(2,5)	(2,5)	(2,5)	(2,5)
# 4	(7,10)	(7,10)	(7,10)	(7,10)	(7,10)	(7,10)	(7,10)	(7,10)	(7,10)	(7,10)	(7,10)	(7,10)
# 5	(1,4)	(1,4)	(1,4)	(1,4)	(1,4)	(1,4)	(1,4)	(1,4)	(1,4)	(1,4)	(1,4)	(1,4)
# 6	(2,8)	(2,8)	(2,8)	(2,8)	(2,8)	(2,8)	(2,8)	(2,8)	(2,8)	(2,8)	**(3,10)**	**(3,10)**
# 7	(8,11)	(8,11)	(8,11)	(8,11)	(4,7)	(4,7)	(1,5)	(1,5)	(1,5)	**(3,10)**	(2,8)	(1,5)
# 8	(4,7)	(4,7)	(4,7)	(4,7)	(8,11)	(1,5)	(4,7)	(4,7)	**(3,10)**	(1,5)	(1,5)	(2,8)
# 9	(1,11)	(1,5)	(1,5)	(1,5)	(1,5)	(8,11)	(8,11)	**(3,10)**	(4,7)	(4,7)	(4,7)	(4,7)
# 10	(1,5)	(1,11)	(1,11)	**(3,10)**	**(3,10)**	**(3,10)**	**(3,10)**	(8,11)	(8,11)	(8,11)	(8,11)	(8,11)
# 11	**(3,10)**	**(3,10)**	**(3,10)**	(1,11)	(1,11)	(1,11)	(1,11)	(1,11)	(1,11)	(1,11)	(1,11)	(1,11)

TABLE 3
Node betweenness ranking in the Abilene network for all θ's.

Rank # 1	# 2	# 3	# 4	# 5	# 6	# 7	# 8	# 9	# 10	# 11
Kansas City	Indianapolis	Denver	Atlanta	Sunnyvale	Houston	Chicago	Los Angeles	New York	Washington	Seattle

a set of linear equations, and yields an efficient process to compute the entire routing continuum and the optimal flow $X^*(\theta)$ for any $\theta \geq 0$. Last but not the least, we remark that although we only focus on network routing in this paper, we believe that our results can be applied to many other applications where the problems can be cast in terms of flows in a network.

Another line of works that is related to our study is parametrized dissimilarity measure (or distance) between nodes. Yen *et al.* [32] develop a family of link-based dissimilarity measures, namely, the randomized shortest-path (RSP) dissimilarity, which generalizes both the weighted shortest path distance and the resistance distance. It is interpreted as the path probability distribution that minimizes the expected energy for transiting from a source node to a destination node, constrained by a fixed relative entropy (Kullback-Leibler divergence) with respect to the reference probability. Chebotarev [12] introduces a similar parametric family of node distance to [32] by matrix forest theorem and the transition inequality, which possess a unique graph-geodetic property: $d(i, j) + d(j, k) = d(i, k)$ if and only if every path from i to k passes through j. Different from our work, the constraints exploited in these works are no longer flow conservation law, thus the solutions obtained have different interpretations of the underlying "flow".

Various algorithms have been proposed to identify the potential based "all-paths" and the shortest paths for a given node pair in the literature. The former [21] requires solving a linear equation system [29] with $O(n^3)$, where n is the total number of nodes in the graph. On the other hand, Dijkstras algorithm [15] and Bellman-Ford algorithm [7] were introduced to compute shortest paths between a node pair in a time complexity of $O(n^2)$ and $O(nm)$ (roughly $O(n^3)$ when the graph is dense), respectively, with m as the total number of edges in the graph. These algorithms aim to extract a routing graph (i.e., the flow distribution) for a particular θ, where our routing continuum algorithm computes the complete set of routing graphs between shortest path routing and "all-path" routing by scanning all possible θ's, thus taking at the worst case $O(n^3m)$. However, in many applications with relatively stable link status, the set of routing graphs do not need to be computed frequently, e.g., in wireless sensor networks with static link transmission delay and energy consumption, and in intradomain administrative network with small chance of link failure. It is interesting to develop more efficient algorithm that can better deal with dynamic link weights, where we leave this as part of our future work.

References

[1] Abilene Project by Internet2 community. *http://www.internet2.edu/abilene/*.

[2] (GN3) GEANT Project. *http://www.geant.net/pages/home.aspx*.

[3] Mit roofnet project. *http://pdos.csail.mit.edu/roofnet/*.

[4] The China Education and Research Network (CERNET). *http://www.edu.cn/cernet_1377/index.shtml*.

[5] Y. Altshuler, R. Puzis, Y. Elovici, S. Bekhor, and A. S. Pentland. Augmented betweenness centrality for mobility prediction in transportation networks. In *NEMO' 11: Proceedings of the international workshop on finding patterns of human behaviors in network and mobility data*, 2011.

[6] J. M. Anthonisse. The rush in a directed graph. *Technical Report BN 9/71, Stichting Mathematisch Centrum, Amsterdam*, 1971.

[7] R. Bellman. On a routing problem. *Quarterly of Applied Mathematics*, 16:87–90, 1958.

[8] S. Borgatti and M. Everett. A graph-theoretic perspective on centrality. *Social networks*, 28(4):466–484, 2006.

[9] U. Brandes and T. Erlebach. *Network analysis: methodological foundations*, volume 3418. Springer, 2005.

[10] U. Brandes and D. Fleischer. Centrality measures based on current flow. *STACS 2005*, pages 533–544, 2005.

[11] E. J. Candes and M. B. Wakin. An Introduction To Compressive Sampling. *IEEE Signal Processing Magazine*, 25(2):21–30, March 2008.

[12] P. Chebotarev. A class of graph-geodetic distances generalizing the shortest-path and the resistance distances. *Discrete Applied Mathematics*, 159(5):295–302, 2011.

[13] S. Cheshire. Latency survey results (for "it's the latency, stupid"), 1996.

[14] A. Cuzzocrea, A. Papadimitriou, D. Katsaros, and Y. Manolopoulos. Edge betweenness centrality: A novel algorithm for qos-based topology control over wireless sensor networks. *Journal of Network and Computer Applications*, 35(4):1210–1217, 2012.

[15] E. W. Dijkstra. A note on two problems in connexion with graphs. *Numerische mathematik*, 1:269–271, 1959.

[16] L. C. Freeman. A set of measures of centrality based on betweenness. *Sociometry*, 40(1):35–41, March 1977.

[17] L. C. Freeman. Centrality in social networks conceptual clarification. *Social Networks*, 1(3):215–239, 1979.

[18] M. Girvan and M. Newman. Community structure in social and biological networks. *Proceedings of the National Academy of Sciences*, 99(12):7821–7826, 2002.

[19] G. Grossi and F. Pedersini. Hub-betweenness analysis in delay tolerant networks inferred by real traces. In *Modeling and Optimization in Mobile, Ad Hoc and Wireless Networks (WiOpt), 2010 Proceedings of the 8th International Symposium on*, pages 318–323. IEEE, 2010.

[20] L. Katz. A new index derived from sociometric data analysis. *Psychometrika*, 18:39–43, 1953.

[21] F. P. Kelly. Network routing. *Philosophical Transactions of the Royal Society*, A(337):343–367, 1991.

[22] Y. Li, Z.-L. Zhang, and D. Boley. The routing continuum from shortest-path to all-path: A unifying theory. In *ICDCS '11: Proceedings of the 31st International Conference on Distributed Computing Systems*, pages 847–856. IEEE, 2011.

[23] M. Newman and M. Girvan. Finding and evaluating community structure in networks. *Physical review E*, 69(2):026113, 2004.

[24] M. E. J. Newman. A measure of betweenness centrality based on random walks. *Social Networks*, 27(1):39–54, January 2005.

[25] M. E. J. Newman. *Networks: An Introduction*. Oxford University Press, 1st edition, 2010.

[26] K. Okamoto. *Fundamentals of optical waveguides*. Academic press, 2010.

[27] L. Page, S. Brin, R. Motwani, and T. Winograd. The pagerank citation ranking: Bringing order to the web. *Technical report, Stanford University*, 1998.

[28] G. Sabidussi. The centrality index of a graph. *Psychometrika*, 31:581–603, 1966.

[29] W. J. Stewart. Numerical methods for computing stationary distributions of finite irreducible markov chains. *Computational Probability*, pages 81–111, 1999.

[30] R. Tibshirani. Regression shrinkage and selection via the lasso. *Journal of the Royal Statistical Society (Series B)*, 58:267–288, 1996.

[31] Y. Tsaig and D. L. Donoho. Compressed sensing. *IEEE Transactions on Information Theory*, 52:1289–1306, 2006.

[32] L. Yen, M. Saerens, A. Mantrach, and M. Shimbo. A family of dissimilarity measures between nodes generalizing both the shortest-path and the commute-time distances. In *Proceeding of the 14th ACM SIGKDD international conference on Knowledge discovery and data mining*, pages 785–793. ACM, 2008.

[33] K. Yoshida, Y. Kikuchi, M. Yamamoto, Y. Fujii, K. Nagami, I. Nakagawa, and H. Esaki. Inferring pop-level isp topology through end-to-end delay measurement. *Passive and Active Network Measurement*, pages 35–44, 2009.